Organic & Biomolecular Chemistry

This article is part of the

OBC 10th anniversary

themed issue

All articles in this issue will be gathered together online at

www.rsc.org/OBC10

Organic & Biomolecular Chemistry

Dynamic Article Links
View Online

Cite this: *Org. Biomol. Chem.*, 2012, **10**, 6022

www.rsc.org/obc

PAPER

Steric desolvation enhances the effective molarities of intramolecular H-bonding interactions†‡

Elena Chekmeneva, Christopher A. Hunter,* Maria Cristina Misuraca and Simon M. Turega

Received 21st February 2012, Accepted 27th March 2012
DOI: 10.1039/c2ob25372k

Free energy contributions due to intramolecular phosphonate diester–phenol H-bonds have been measured for 20 different supramolecular architectures in cyclohexanone solution. High throughput UV/Vis titrations were used in combination with chemical double mutant cycles to dissect out the contributions of different functional group interactions to the stabilities of over 100 different zinc porphyrin–pyridine ligand complexes. These complexes have previously been characterised in toluene and in 1,1,2,2-tetrachloroethane (TCE) solution. Intramolecular ester–phenol H-bonds that were measured in these less polar solvents are too weak to be detected in cyclohexanone, which is a more competitive solvent. The stability of the intermolecular phosphonate diester–phenol H-bond in cyclohexanone is an order of magnitude lower than in TCE and two orders of magnitude lower than in toluene. As a consequence, only seven of the twenty intramolecular phosphonate diester–phenol interactions that were previously measured in toluene and TCE could be detected in cyclohexanone. The effective molarities (EM) for these intramolecular interactions are different in all three solvents. Determination of the EM accounts for solvent effects on the strengths of the individual H-bonding interactions and the zinc porphyrin–pyridine coordination bond, so the variation in EM with solvent implies that differences in the solvation shells make significant contributions to the overall stabilities of the complexes. The results suggest that steric effects lead to desolvation of bulky polar ligands. This increases the EM values measured in TCE, because ligands that fail to replace the strong interactions made with this solvent are unusually weakly bound compared with ligands that make intramolecular H-bonds.

Introduction

Synthetic supramolecular complexes provide the ideal platform for exploring the fundamentals of non-covalent chemistry in relatively simple well-defined systems. Synthetic constructs have been used to measure functional group interactions,[1] long range secondary interactions,[2] the role of desolvation,[3] and cooperative effects in multivalent systems.[4] The results have a direct bearing on processes that range from the structures of biomacromolecules to the properties of molecular materials and the development of new catalysts.[5] Supramolecular complexes also provide well-characterised tractable systems for benchmarking molecular simulation methods for making predictions of the structures and thermodynamic properties of non-covalent systems.[6]

Department of Chemistry, University of Sheffield, S3 7HF, UK. E-mail: C.Hunter@shef.ac.uk; Fax: +44 114 2229346; Tel: +44 114 2229476

†Electronic supplementary information (ESI) available: Details of the partially bound states analysis, statistical factors σ, values of K EM, H-bond occupancy. See DOI: 10.1039/c2ob25372k

‡This article is part of the *Organic & Biomolecular Chemistry* 10th Anniversary issue.

We have been developing methods for quantifying functional group interactions in cooperative recognition interfaces that interact *via* multiple contacts.[7] Although it is possible to make reasonably accurate predictions of the stabilities of simple complexes that are held together by single point interactions like H-bonds,[8] systems that make multiple non-covalent contacts are less well-understood. In addition, the effect of solvent on such processes is an area that is largely unexplored, and development of reliable models for understanding solvation in complex systems represents a major challenge for supramolecular chemistry.[9] This paper describes a quantitative investigation of solvent effects on chelate cooperativity.

Approach

Metalloporphyrin–ligand complexes of the type shown in Fig. 1 provide an ideal platform for systematic studies of chelate cooperativity in a relatively complicated but tractable molecular recognition interface.[7] Chemical double mutant cycles (DMC) can be used to dissect out the free energy contributions due to individual H-bonding interactions in these systems.[10] The approach is illustrated in Fig. 2. By comparing the properties of

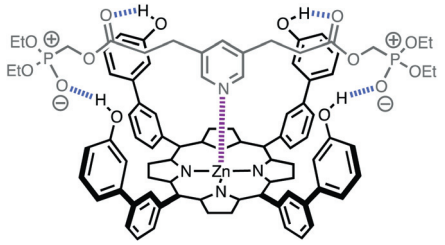

Fig. 1 Structure of a complex formed between a zinc porphyrin (black) and a pyridine ligand (grey), which forms four intramolecular H-bonds (blue).

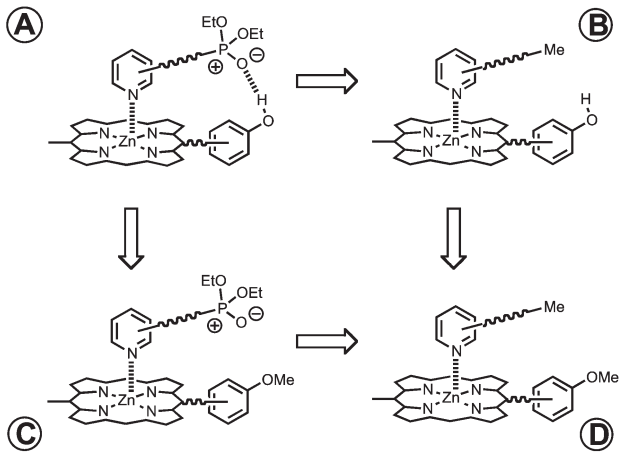

Fig. 2 Chemical double mutant cycle (DMC) for measurement of the free energy contribution of the phosphonate diester–phenol H-bond to the stability of complex A.

single mutants (complexes B and C) with the double mutant (complex D), it is possible to measure all secondary interactions between the H-bonding groups and the core zinc porphyrin–pyridine units. Thus eqn (1) gives the free energy contribution ($\Delta\Delta G°$) due to the phosphonate diester–phenol H-bond in complex A in Fig. 2 without any contribution from these secondary interactions. Experimental measurement of the free energies of intramolecular H-bonding interactions as a function of porphyrin and ligand geometry provides insight into the relationship between supramolecular architecture and the magnitude of chelate cooperativity in these systems.

$$\Delta\Delta G° = \Delta G_A° - \Delta G_B° - \Delta G_C° + \Delta G_D° \quad (1)$$

We have previously reported experiments on a family of closely-related complexes where this analysis was applied to 48 different recognition interfaces involving zinc porphyrin–pyridine coordination, phosphonate diester–phenol H-bonds, ester–phenol H-bonds and ether–phenol H-bonds.[7] These measurements of chelate cooperativity were carried out in toluene and in TCE solutions. Although the difference in polarity is rather subtle, changing the solvent from toluene to TCE had a surprisingly large effect on the effective molarities for the intramolecular interactions in these systems.[7b] In an attempt to understand the origin of this solvent effect on chelate cooperativity, we have investigated the same systems in a significantly more polar solvent, cyclohexanone. This paper reports experiments in this solvent and compares the results with the data obtained in toluene and TCE.

Results and discussion

Figs. 3 and 4 show the porphyrins and ligands used to investigate solvent effects on chelate cooperativity. The synthesis of

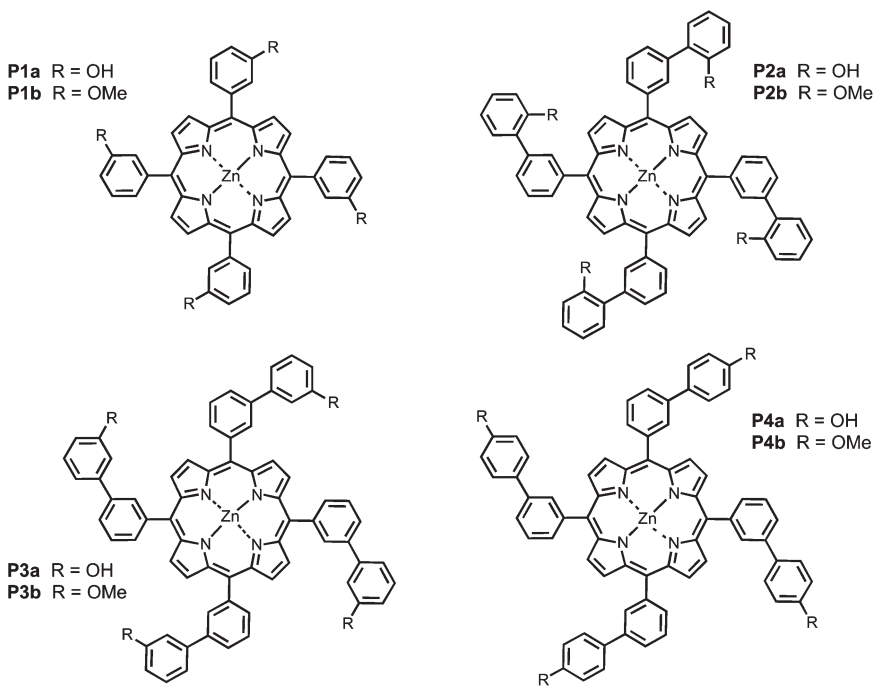

Fig. 3 Zinc porphyrin receptors **P1a–P4a** (R = OH) and **P1b–P4b** (R = OMe).

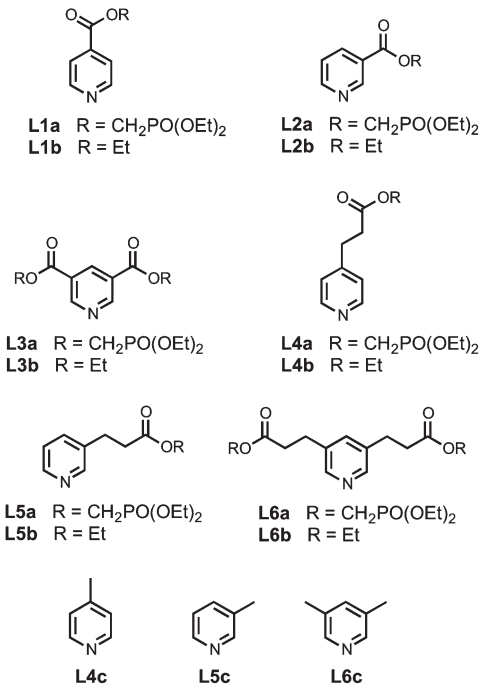

Fig. 4 Phosphonate diester ligands, **L1a–L6a**, ester ligands, **L1b–L6b**, and control ligands with no H-bonding groups, **L4c–L6c**.

these compounds was described previously.[7] Four of the zinc porphyrin receptors are equipped with four phenol H-bond donor sites located at different positions around the periphery of the metal binding site, **P1a–P4a** (Fig. 3). The corresponding methoxy porphyrins, **P1b–P4b**, serve as control compounds that can not make H-bonds. The ligands are all based on pyridine carboxylic acids that allow attachment of up to four H-bonding groups at various positions on the ligand. Ligands **L1a–L6a** are equipped with phosphonate diester groups, and the corresponding ethyl ester ligands, **L1b–L6b**, serve as controls for the construction of DMCs for the measurement of phosphonate diester–phenol H-bonds. Ligands **L4c**, **L5c** and **L6c** are used as non H-bonding mutants for construction of DMCs for the measurement of ester–phenol H-bonds. Previous work showed that intramolecular H-bonding interactions are at the limit of detection for ligand **L1a** in TCE.[7b] As we will see, the H-bonding interactions are much weaker in cyclohexanone, so **L1a** and **L1b** are excluded from this study.

Solvent effects on intermolecular H-bonding

Cyclohexanone is a significantly more polar solvent than toluene and TCE (Table 1). In particular, the H-bond acceptor parameter β of cyclohexanone is much higher which means that the phenol H-bond donor groups will be more strongly solvated in cyclohexanone. The effect on the stability of intermolecular phosphonate diester–phenol H-bonds was measured experimentally using the compounds shown in Fig. 5 and ^{1}H NMR titrations in d_2-TCE, d_8-toluene and d_{10}-cyclohexanone (K_{ref} in Table 1). It is also possible to estimate the values of intermolecular association constants for the formation of complexes involving a single H-bond using eqn (2) (K_{calc} in Table 1).[8a]

Table 1 H-bond parameters and association constants (M^{-1}) for the formation of intermolecular complexes measured by ^{1}H NMR titrations in d_{10}-cyclohexanone, d_2-TCE and in d_8-toluene at 298 K (K_{ref}) and calculated using eqn (2) (K_{calc})[a]

Solvent	Complex	α_D	β_A	α_S	β_S	K_{ref}	K_{calc}
Cyclohexanone	**7·8**	3.8	5.4	1.5	5.8	[b]	0.06
TCE	**7·8**	3.8	5.4	2.0	1.3	2 ± 1	2
Toluene	**7·8**	3.8	5.4	1.0	2.2	3 ± 1	3
Cyclohexanone	**7·9**	3.8	8.9	1.5	5.8	3 ± 1	2
TCE	**7·9**	3.8	8.9	2.0	1.3	13 ± 1	23
Toluene	**7·9**	3.8	8.9	1.0	2.2	140 ± 10	180

[a] H-bond parameters from ref. 8. [b] This complex is not sufficiently stable to determine the association constant in cyclohexanone.

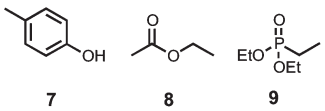

Fig. 5 Compounds used to measure K_{ref}, the association constant for the formation of intermolecular H-bonds.

$$-RT \ln K_{calc} = -(\alpha_D - \alpha_S)(\beta_A - \beta_S) + 6 \text{ kJ mol}^{-1} \quad (2)$$

where K_{calc} is the intermolecular association constant at T = 298 K, α_D and β_A are the H-bond parameters of the H-bond donor (D) and H-bond acceptor (A), α_S and β_S are the H-bond donor and acceptor parameters of the solvent, and the constant of 6 kJ mol^{-1} was experimentally determined in carbon tetrachloride solution.[8]

H-bonding interactions between **7** and **8** could not be detected in cyclohexanone solution, and this is consistent with the very low association constant predicted by eqn (2). Although some of the association constants in Table 1 are too low to be measured with a high degree of accuracy, the values of K_{calc} are all in good agreement with the experimental values of K_{ref}, which provides confidence in the reliability of the values of the intermolecular association constants in Table 1. The phosphonate diester–phenol H-bond in cyclohexanone is an order of magnitude less stable than in TCE and two orders of magnitude less stable than in toluene. The phosphonate diester is such a strong H-bond acceptor that it can compete effectively with a polar solvent like cyclohexanone for interactions with H-bond donors, whereas the carboxylic acid ester is a much weaker H-bond acceptor and can not.

High throughput titration analysis of binding

The association constants for all porphyrin–ligand combinations were measured using a UV/Vis plate-reader that allows routine determination of large numbers of association constants. The zinc porphyrins have an intense UV/Vis absorption band at 420 nm, which shifts by around 10 nm when a pyridine ligand binds to the zinc, and this provides a convenient spectroscopic probe of binding. The titration data fit well to a 1 : 1 binding isotherm in all cases, and the results are collected in Table 2. The stability of the complexes in cyclohexanone is low. This leads to

Table 2 Association constants (K/M^{-1}) for the formation of 1 : 1 complexes measured using UV/Vis titrations in cyclohexanone at 298 K (with percentage errors at the 95% confidence limit based on multiple repeats of the measurement)

	Porphyrin							
Ligand	**P1a**	**P2a**	**P3a**	**P4a**	**P1b**	**P2b**	**P3b**	**P4b**
L2a	1.5×10^2 (45%)	6.7×10^1 (40%)	2.3×10^2 (16%)	5.8×10^1(17%)	5.8×10^1 (58%)	3.6×10^1 (35%)	5.1×10^1 (25%)	6.3×10^1 (36%)
L3a	5.4×10^1 (52%)	2.3×10^1 (32%)	4.9×10^1 (30%)	3.4×10^1 (34%)	[a]	[a]	[a]	[a]
L4a	7.7×10^2 (14%)	7.3×10^2 (16%)	6.7×10^2 (6%)	5.9×10^2 (4%)	3.9×10^2 (28%)	3.5×10^2 (12%)	3.7×10^2 (4%)	3.6×10^2 (14%)
L5a	7.7×10^2 (4%)	9.3×10^2 (14%)	5.0×10^2 (8%)	5.9×10^2 (8%)	1.3×10^2 (41%)	2.1×10^2 (7%)	1.9×10^2 (9%)	2.4×10^2 (34%)
L6a	2.9×10^2 (14%)	4.7×10^2 (14%)	2.4×10^2 (4%)	1.9×10^2 (6%)	1.1×10^2 (14%)	9.7×10^1 (8%)	9.7×10^1 (2%)	1.1×10^2 (2%)
L2b	6.3×10^1 (38%)	9.7×10^1 (26%)	8.2×10^1 (30%)	1.2×10^2 (20%)	6.9×10^1 (35%)	6.2×10^1 (14%)	9.4×10^1 (15%)	7.6×10^1 (2%)
L3b	2.9×10^1 (38%)	2.9×10^1 (36%)	4.6×10^1 (33%)	3.3×10^1 (35%)	2.6×10^1 (55%)	2.6×10^1 (59%)	2.8×10^1 (66%)	3.2×10^1 (34%)
L4b	5.8×10^2 (20%)	5.8×10^2 (4%)	5.3×10^2 (21%)	5.0×10^2 (28%)	4.6×10^2 (24%)	4.8×10^2 (6%)	5.2×10^2 (12%)	5.0×10^2 (12%)
L5b	2.0×10^2 (48%)	4.5×10^2 (10%)	4.2×10^2 (14%)	3.6×10^2 (16%)	1.8×10^2 (10%)	2.5×10^2 (39%)	2.8×10^2 (20%)	2.5×10^2 (14%)
L6b	1.1×10^2 (14%)	3.0×10^2 (38%)	2.8×10^2 (24%)	2.9×10^2 (16%)	1.2×10^2 (20%)	1.8×10^2 (14%)	1.8×10^2 (10%)	1.9×10^2 (10%)
L4c	6.3×10^2 (6%)	6.4×10^2 (8%)	5.7×10^2 (10%)	5.0×10^2 (4%)	5.8×10^2 (23%)	4.2×10^2 (11%)	4.9×10^2 (10%)	4.7×10^2 (12%)
L5c	1.9×10^2 (8%)	2.2×10^2 (8%)	1.9×10^2 (10%)	1.8×10^2 (2%)	1.3×10^2 (26%)	1.5×10^2 (40%)	1.4×10^2 (12%)	1.5×10^2 (2%)
L6c	2.2×10^2 (4%)	2.7×10^2 (22%)	1.9×10^2 (18%)	1.9×10^2 (12%)	1.6×10^2 (10%)	1.7×10^2 (6%)	1.6×10^2 (14%)	1.6×10^2 (18%)

[a] These complexes are not sufficiently stable for accurate measurement of the association constant.

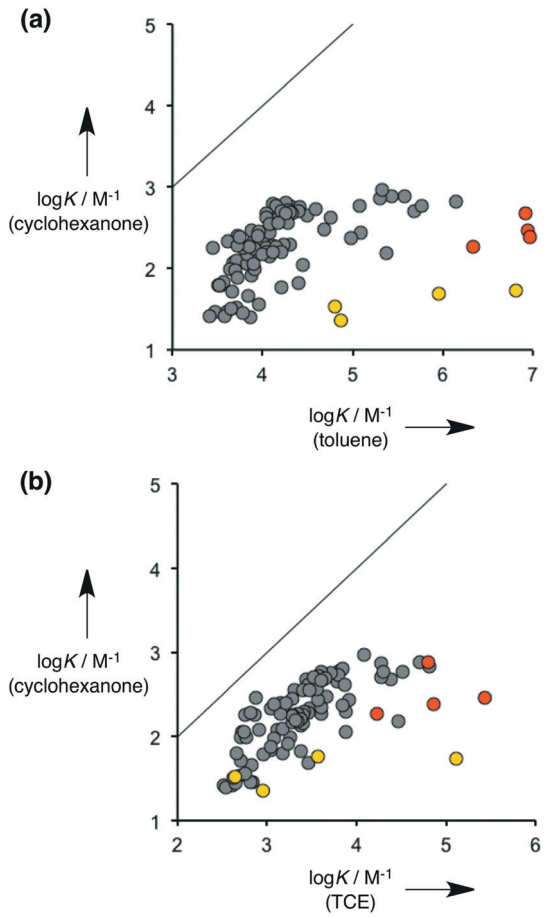

Fig. 6 Comparison of the 1 : 1 association constants (log K/M^{-1}) for porphyrin–ligand complexes in cyclohexanone with the corresponding values measured in (a) toluene and in (b) TCE. Data for the complexes of **L3a** with **P1a–P4a** (yellow) and complexes of **L6a** with **P1a–P4a** (red) are highlighted. The lines correspond to log K (toluene) = log K (cyclohexanone) and log K (TCE) = log K (cyclohexanone).

relatively large errors, and the complexes of **L3a** with **P1b–P4b** were not sufficiently stable to determine association constants.

Fig. 6 compares the association constants measured in cyclohexanone with those reported previously in toluene (Fig. 6a) and in TCE (Fig. 6b).[7] The association constants in cyclohexanone are three to four orders of magnitude lower than in toluene and one to two orders of magnitude lower than in TCE. In toluene and TCE, the values of log K span a wide range due variation in the contributions from intramolecular H-bonding interactions. The range of values in cyclohexanone is significantly narrower, because cyclohexanone competes with both the zinc–pyridine and the H-bond interactions. The most stable complexes in toluene and TCE have larger contributions due to intramolecular H-bonds, and so they are more strongly affected by changing the solvent to cyclohexanone.

In general, there is a reasonable correlation between the association constants measured in the three solvents, but there are some outliers. The outliers highlighted in Fig. 6a are the complexes of **L3a** with **P1a–P4a** (yellow) and **L6a** with **P1a–P4a** (red). These complexes are also highlighted in Fig. 6b, where there are fewer discrepancies. We have previously noted that the properties of the **L3a** and **L6a** complexes are different in toluene and TCE. The complexes of these ligands with **P1b–P4b**, which can not make intramolecular H-bonds, also gave anomalously low association constants in TCE, and this suggests that steric effects may be significant for these ligands. Data for the complexes formed between **L3a** and **P1b–P4b** are missing from Fig. 6, because these complexes were not sufficiently stable to allow determination of association constants, which suggests that the behaviour in cyclohexanone is similar to TCE.

DMC analysis of intramolecular H-bonding

Fig. 7 shows the data in Table 2 with the complexes organised according to their role in the DMC used to measure intramolecular phosphonate diester–phenol H-bonds. In general, the complexes that can make phosphonate diester–phenol H-bonds (complex A, blue data in Fig. 7) are more stable than the other complexes.

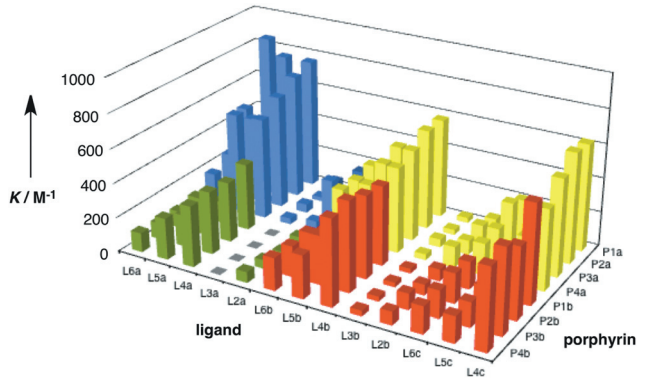

Fig. 7 Association constants (K/M^{-1}) for formation of 1 : 1 complexes (phosphonate ligand–hydroxyporphyrin complexes in blue, phosphonate ligand–methoxyporphyrin complexes in green, control ligand–hydroxyporphyrin complexes in yellow, control ligand–methoxyporphyrin complexes in red).

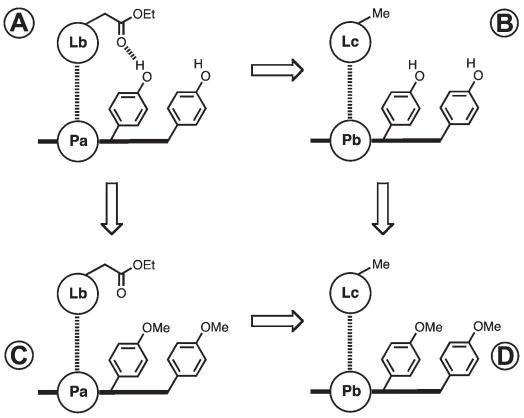

Fig. 8 DMC for evaluating the thermodynamic contribution of ester–phenol H-bonds to the stability of a porphyrin–ligand complex.

Ester–phenol H-bonds. Fig. 8 shows the DMC used to measure the free energy contributions due to intramolecular ester–phenol H-bonds. In toluene and TCE, H-bonding to the ester groups contributes up to 6 kJ mol^{-1} to the overall stability of a complex, but in cyclohexanone, the values of $\Delta\Delta G°$ from the DMC analysis were all 0 ± 1 kJ mol^{-1}. This is consistent with the data for intermolecular ester–phenol H-bonds in Table 1, which suggests that the ester is not sufficiently polar to compete with cyclohexanone for H-bonding interactions.

Phosphonate diester–phenol H-bonds. Fig. 9 shows the DMC used to measure the free energy contributions due to phosphonate diester–phenol H-bonds. Although we were not able to reliably quantify ester–phenol H-bonding interactions using the DMC in Fig. 8, the DMC in Fig. 9 factors out any small contributions due to interactions with the ester groups, and this allows measurement of the phosphonate diester–phenol interactions in the presence of ester–phenol interactions. The results are summarised in Table 3. Accurate values for ligand **L3a** are not available, because the association constants for the interaction of **L3a** with **P1b**–**P4b**, complex C in the DMC, were too low to be measured reliably. However, it is possible to obtain approximate

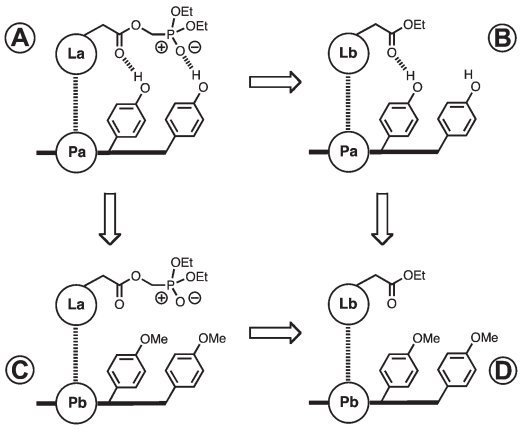

Fig. 9 DMC for evaluating the thermodynamic contribution of phosphonate diester–phenol H-bonds to the stability of a porphyrin–ligand complex.

Table 3 Total free energy contributions due to phosphonate diester–phenol H-bonding interactions ($\Delta\Delta G°$/kJ mol^{-1}) determined using the chemical double mutant cycle in Fig. 9 and data obtained at 298 K in cyclohexanone. Complexes that do not make detectable H-bonds are shaded[a]

	ligand				
porphyrin	**L2a**	**L3a**[b]	**L4a**	**L5a**	**L6a**
P1a	-4	-2	-1	-4	-2
P2a	0	1	-1	-2	-3
P3a	-4	0	-1	-1	-1
P4a	1	0	-1	-1	0

[a] Average error over the data set ± 1 kJ mol^{-1}. [b] These values were estimated using $\Delta G_A° - \Delta G_B°$ rather than the full DMC.

values for these interactions by using the top arm of the DMC, *i.e.* $\Delta G_A° - \Delta G_B°$, and these values are quoted in Table 3.

Only seven of the twenty different supramolecular architectures studied show detectable H-bonding interactions (Table 3). This result is very different from the results in toluene and TCE, where H-bonding could be measured in all twenty complexes. Solvent competition clearly has a dramatic effect on intramolecular H-bonding in these systems. Comparison of the results for ligands that have two symmetrical side arms (**L3a** and **L6a**) with the corresponding one-armed ligands (**L2a** and **L5a**) reveals some interesting features in the data in the Table 4. In toluene, the free energy contributions due to H-bonding for the two-armed ligands are double those for the one-armed ligands. This implies that the two-armed ligands make two identical H-bonds. In cyclohexanone, this is clearly not the case. With the exception of the **L6a**·**P2a** complex, the free energy contributions due to H-bonding are actually lower for the two-armed ligands compared with the one-armed ligands. In other words, addition of the second side arm destabilises the complexes in cyclohexanone. Similar effects were observed in TCE,[7b] and as explained above, it is possible that the discrepancies may be due to adverse steric interactions in the complexes involving the bulkiest ligands, **L3a** and **L6a**.

Table 4 Values of $\Delta G_C^\circ - \Delta G_D^\circ$ for the DMC in Fig. 9 (kJ mol^{-1}). Complexes where there is no detectable difference in free energy are shaded[a]

		ligand				
solvent	porphyrin	L2a	L3a	L4a	L5a	L6a
toluene	P1a	-2	-2	0	1	-1
toluene	P2a	-2	0	0	1	-1
toluene	P3a	0	-1	0	1	-1
toluene	P4a	1	0	0	1	-1
TCE	P1a	2	3	0	1	1
TCE	P2a	2	2	0	1	0
TCE	P3a	2	4	0	1	1
TCE	P4a	2	3	0	1	0
cyclohexanone	P1a	2	[b]	0	1	0
cyclohexanone	P2a	2	[b]	1	0	2
cyclohexanone	P3a	2	[b]	1	1	2
cyclohexanone	P4a	0	[b]	1	0	1

[a] Average error over the data set ±1 kJ mol^{-1}. [b] Association constants for complex C were too low to be measured reliably for **L3a** in cyclohexanone.

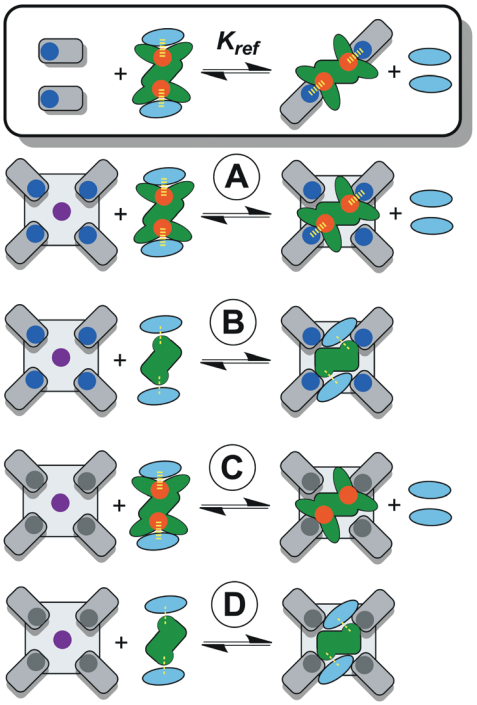

Fig. 10 Desolvation of porphyrin–ligand complexes. The complexes are labelled according to their role in the DMC in Fig. 9. The porphyrin receptors are grey, the ligands are green and solvent is pale blue. The H-bonding sites are red on the ligand, dark blue on the porphyrin and the corresponding non H-bonding mutant sites are shown as green and grey circles respectively. Binding of **L3a** to **P1b** in TCE involves fitting a sterically demanding ligand into the binding pocket (complex **C**), and this leads to partial desolvation of the phosphonate diester groups. In complex A of the DMC, interactions of the phosphonate diester groups with TCE in the free state are replaced by H-bonds with the phenol groups. Complexes **B** and **D** involve the smaller control ligand, **L3b**, so changes in the solvation shell are less dramatic. The top box shows that the intermolecular binding interaction used to measure K_{ref} involves the same desolvation process as formation of complex **A**, which cancels out in the calculation of EM. However, desolvation of the phosphonate diester groups on formation of complex **C** does not cancel out in this analysis and leads to an anomalously high value of EM in TCE.

It is possible to obtain an estimate of the magnitude of potential steric interactions, by comparing complexes C and D in the DMC in Fig. 9. These complexes can not make intramolecular H-bonds, so the difference $\Delta G_C^\circ - \Delta G_D^\circ$ is dominated by secondary effects, like changes in solvation and steric interactions. Table 4 shows the values for the phosphonate diester ligands in the three different solvents. In most cases, the values are close to or within the experimental error. However, there are consistent differences for all of the complexes involving **L2a** and **L3a** in TCE. A positive value of the free energy difference in Table 4 means that addition of the phosphonate diester group destabilises the complex. **L2a** and **L3a** are the ligands that position the phosphonate diester groups closest to the central core of the complex, so they are expected to show the largest steric effects. The effects do not depend on the structure of the porphyrin but do depend on the solvent. The values are roughly twice as large for the two armed ligand, **L3a**, compared with the one-armed ligand, **L2a**, which is consistent with an additive effect associated with solvation of the phosphonate diester groups in TCE.

Fig. 10 shows a possible explanation. TCE is a better H-bond donor than the other two solvents (Table 1), and strong solvation of the phosphonate diester by TCE significantly increases the effective size of the ligand. Disruption of these solvent interactions may be required for binding to **P1b–P4b** (complex C in Fig. 10). When **L2a** and **L3a** bind to **P1a–P4a**, the interactions with solvent are replaced by H-bonding interactions with the phenol groups (dark blue sites in complex A in Fig. 10). Comparison of complexes A and C in effect measures H-bonding interactions with a phosphonate diester that is partially desolvated. The evaluation of EM below compares the properties of complexes A, B, C and D in Fig. 10 with the intermolecular H-bonding interactions given by K_{ref}. Desolvation of the phosphonate diester groups in the intermolecular process involves the same process as in formation of complex A, so these contributions cancel out in the evaluation of EM. However, desolvation of the phosphonate diester groups in complex C does not cancel out and makes an additional contribution to the value of EM. The result is that the values of EM measured for **L2a** and **L3a** in TCE are unusually high, because they contain a contribution from ligand desolvation in complex C. A TCE–phosphonate diester CH·O H-bond is worth 18 kJ mol^{-1} according to the H-bond parameters in Table 1 ($\alpha_S\beta_D$), so the effects of this phenomenon are potentially large.

Returning to the data in Table 3, there are two interpretations of the small values of $\Delta\Delta G^\circ$ observed for the two-armed ligands: either the two-armed ligand makes one H-bond of a similar strength to the one-armed ligand, or the two-armed ligand makes two weaker H-bonds. These possibilities can be distinguished using ^{1}H NMR spectroscopy. The signals due to the porphyrin pyrrole protons provide a sensitive probe of the number of intramolecular H-bonds formed in a complex.[7b] For ligands that make only one H-bond, the pyrrole signals of the complex are singlets, but if more than one H-bond is made, splitting of the

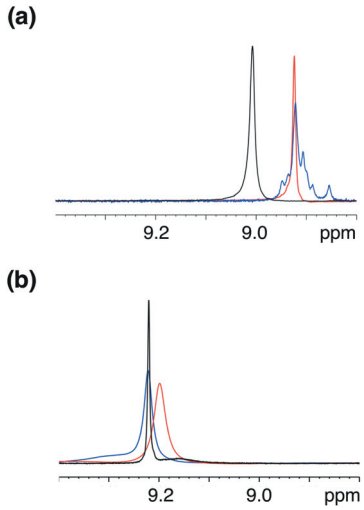

Fig. 11 Pyrrole region of 400 MHz ^{1}H NMR spectra of free **P1a** (black), 1 : 1 mixtures with the one-armed ligand, **L5a** (red), and the two-armed ligand, **L6a** (blue), recorded at mM concentrations in d_2-TCE (a) and in d_{10}-cyclohexanone (b).

pyrrole signal is observed due to slow exchange between the six different types of atropisomer that make different interactions with the ligand. Fig. 11 compares the ^{1}H NMR spectra of the **P1a·L5a** and **P1a·L6a** complexes recorded in TCE and in cyclohexanone. In TCE, the **P1a·L6a** complex makes two H-bonds, and the pyrrole signal accordingly appears as a multiplet. In cyclohexanone, no splitting is observed, which implies that the two-armed ligand, **L6a**, does not make a second H-bond with **P1a**.

Effective molarities

By comparing the intermolecular association constants measured for the reference compounds in Table 1 with the free energy contributions due to intramolecular H-bonding in the porphyrin–ligand complexes in Table 3, it is possible to determine the effective molarities (EM) for the intramolecular processes.[11] Fig. 12 illustrates the relevant equilibrium for a complex that makes one intramolecular H-bond. The bound state is a population weighted distribution of the fully bound complex, where the zinc–nitrogen and phosphonate diester–phenol interactions are both made, and the partially bound state, where only the coordination bond is made. The other partially bound state, where the coordination bond is broken and the H-bond is formed, is not populated to any significant extent in these systems, because the coordination bond is so much stronger than the H-bond (see Tables 1 and 2). Thus the observed association constant for the complex in Fig. 1 is given by eqn (3).

$$K_{obs} = (1 + K_{ref}EM)K_0 \quad (3)$$

where K_0 is the intermolecular association constant for porphyrin–ligand coordination, K_{ref} is the association constant for formation of the corresponding intermolecular H-bond, and EM is the effective molarity for the intramolecular interaction.

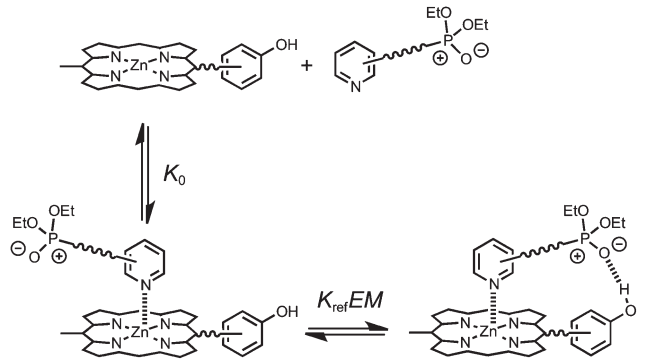

Fig. 12 Stepwise equilibria in the formation of a porphyrin–pyridine complex containing an intramolecular phosphonate diester–phenol H-bond. K_0 is the intermolecular association constant for formation of the zinc–nitrogen interaction. K_{ref}EM is the equilibrium constant for formation of the intramolecular H-bond. K_{ref} is the equilibrium constant for formation of the corresponding intermolecular H-bond. EM is the effective molarity for the intramolecular interaction.

This expression can be generalised to complexes where multiple intramolecular H-bonds are possible by summing over all possible bound states (eqn (4) and (5)).

$$K_{obs} = fK_0 \quad (4)$$

where

$$f = 1 + \sum_i \sigma_i K_i EM_i + \sum_{i,j}^{N} \sigma_{ij} K_i EM_i K_j EM_j + \ldots + \sigma_{ij\ldots N} \prod_i^N K_i EM_i \quad (5)$$

and K_0 is the intermolecular association constant for formation of the zinc–nitrogen interaction, K_i is the association constant for formation of the relevant intermolecular H-bond, EM_i is the effective molarity for formation of the intramolecular interaction, and σ are statistical factors that describe the degeneracies of the partially and fully bound states.

Differences in the zinc–nitrogen interaction, K_0, from one complex to another, cancel out in the DMC, so the values of EM_i can be related to the experimentally measured value of $\Delta\Delta G^\circ$ by eqn (6).

$$e^{-(\Delta\Delta G^o/RT)} = \frac{f_A f_D}{f_B f_C} \quad (6)$$

The values of K_{ref} in Table 1 were used as K_i in eqn (5), and the DMC free energy differences in Table 3 were used to solve eqn (6) for the values of EM_i for the intramolecular H-bond interactions in all of the complexes (Table 5). The ESI† contains full details of the analysis of the partially bound states and statistical factors, σ, for each DMC. The value of K_{ref} is 3 M^{-1} for the phosphonate diester–phenol H-bond, and EM is less than 1 M for all of the complexes, so there are significant populations of partially bound states in all of these systems.

The calculation of EM factors out any contributions from differences in the properties of the individual H-bonding interactions and should simply reflect the ease with which the system is able to form intramolecular contacts. In other words, the value

Table 5 Effective molarities (EM/mM) for intramolecular phosphonate diester–phenol H-bonds measured at 298 K in cyclohexanone.[a] Complexes that do not make detectable H-bonds are shaded

porphyrin	L2a	L3a	L4a	L5a	L6a
P1a	325	[c]	[b]	415	[c]
P2a	[b]	[b]	[b]	128	68
P3a	378	[b]	[b]	[b]	[b]
P4a	[b]	[b]	[b]	[b]	[b]

[a] Average error over the data set ±50%. [b] These complexes do not make detectable H-bonds. [c] These complexes do not make any additional H-bonds compared with the one-armed ligands **L2a** and **L5a**.

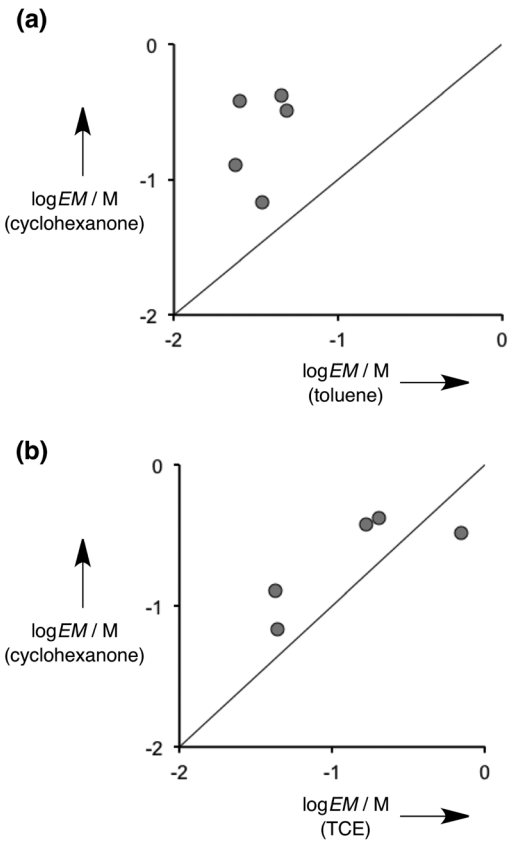

Fig. 13 Comparison of effective molarities (EM) for formation of intramolecular phosphonate diester–phenol H-bonds in cyclohexanone with the corresponding values measured in toluene (a) and in TCE (b). The lines correspond to log EM (cyclohexanone) = log EM (toluene) and log EM (cyclohexanone) = log EM (TCE).

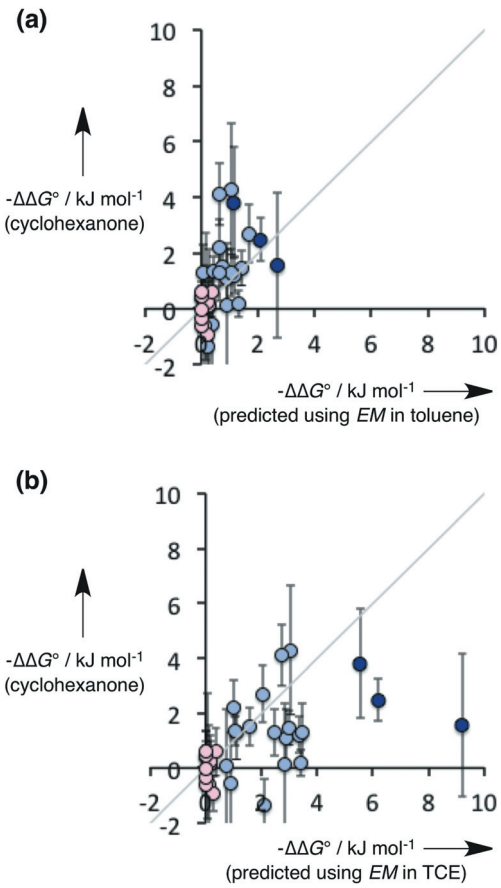

Fig. 14 Comparison of free energy contributions due to intramolecular H-bonds (ΔΔ*G*°) measured experimentally in cyclohexanone and predicted using the values of EM measured in toluene (a) and in TCE (b). Data for ester–phenol H-bonds in red and phosphonate diester–phenol H-bonds in blue. Complexes that are outliers in TCE are highlighted in dark blue on both graphs. The lines correspond to ΔΔ*G*° (experiment) = ΔΔ*G*° (predicted).

of EM might be expected to be a function of the supramolecular architecture and independent of the solvent. This is true for the ester–phenol interactions measured in toluene and TCE,[7b] which are practically identical in the two solvents and show little variation with supramolecular architecture. However, the values of EM for the phosphonate diester–phenol H-bonds measured in TCE span nearly two orders of magnitude and are very different from those measured in toluene. Fig. 13 compares the values of EM measured in cyclohexanone with the corresponding values in toluene and TCE. There is no correlation between the values measured in toluene and cyclohexanone (Fig. 13a). Although there are only five data points, the trends in the values of EM measured in cyclohexanone are similar to TCE (Fig. 13b). There is one outlier in Fig. 13b: the **P1a·L2a** complex has the highest EM of all of the complexes in TCE, but the value in cyclohexanone is significantly lower. The difference may be due to partial desolvation of **L2a** in complex C of the DMC in TCE as illustrated in Fig. 10.

The small number of complexes that gave measurable intramolecular interactions in cyclohexanone raises question marks over the validity of the comparisons in Fig. 13. However, it is possible to compare the experiments in different solvents in a different way. Values of EM were measured in toluene and in TCE for all twenty complexes studied here. These values can be used in conjunction with the values of K_{ref} in Table 1 and eqn (5) and (6) to predict the values of ΔΔ*G*° that would be expected in cyclohexanone, if the values of EM were identical to those found in toluene or in TCE. Fig. 14 shows the results. The ester–phenol interactions (red points) are all predicted to be small in agreement with the experimental results in cyclohexanone. The agreement is less good for the phosphonate diester–phenol

interactions (blue points). The toluene EM values predict relatively small values of $\Delta\Delta G°$ in cyclohexanone (Fig. 14a), and the agreement with the experimental results is reasonable. The TCE EM values generally overestimate the values of $\Delta\Delta G°$ in cyclohexanone, and there are some particularly large discrepancies, **P1a·L3a**, **P1a·L2a** and **P1a·L6a** (dark blue points in Fig. 14b). These complexes have the highest values of EM measured in TCE but this is clearly not the case in the cyclohexanone. The toluene EM values accurately predict the properties of these outliers (dark blue points in Fig. 14a). This implies that the values of EM measured in TCE are anomalous due to partial desolvation of the bulky ligands in complex C of the DMC as illustrated in Fig. 10.

These results show that there are specific solvation effects that contribute as much as 8 kJ mol^{-1} to differences in the stabilities of these complexes. These solvent effects are not related to the properties of the primary functional groups involved in ligand coordination or H-bonding, since these contributions are factored out in the determination of EM. Rather the variations are related to differences in the way in which the complexes as a whole are solvated.

Conclusions

We have used chemical double mutant cycles to quantify intramolecular H-bonding interactions in cyclohexanone. The results are compared with previous experiments on the same complexes in toluene and in TCE. The results show that there are significant solvent effects in these systems. In both toluene and TCE, all twenty of the porphyrin–ligand complexes studied here make intramolecular phosphonate diester–phenol H-bonds, and six of the complexes also make ester–phenol H-bonds. Cyclohexanone is a much more polar solvent and competes more strongly for interactions with the phenol H-bond donors on the porphyrin receptors. As a result, no ester–phenol interactions could be detected in cyclohexanone, and only seven of the twenty complexes gave phosphonate diester–phenol H-bonds that were strong enough to measure. Measurements of intermolecular phosphonate diester–phenol interactions show that this H-bond is an order of magnitude less stable in cyclohexanone compared with TCE and two orders of magnitude less stable compared with toluene, and this accounts qualitatively for the solvent effects on complex stability.

A more detailed analysis used DMCs to determine the contributions of intramolecular H-bonds to the overall stabilities of the porphyrin–ligand complexes. The intermolecular association constants were used to convert these measurements into effective molarities (EM) for the intramolecular interactions. The values of EM measured in cyclohexanone show no correlation with the values measured in toluene but compare well with the values measured in TCE. There are only five data points in cyclohexanone, but the values of EM measured in toluene and TCE can be used to calculate expected stabilities of the complexes in cyclohexanone, assuming that EM is an intrinsic property of the complex and can be transferred between solvents. This allows comparison of all twenty values of $\Delta\Delta G°$ measured in cyclohexanone with the results from toluene and TCE. There is reasonable agreement between the toluene and cyclohexanone data, but there are significant discrepancies for TCE. Differences of up to 8 kJ mol^{-1} are found between the experimental free energy contribution due to intramolecular H-bonding in cyclohexanone and the value estimated based on the EM measured in TCE. The EM values measured in TCE appear to be anomalously high, and this is ascribed high to partial desolvation of the phosphonate diester groups of sterically crowded ligands in complex C of the DMC.

These experiments indicate that there are substantial solvent effects on the value of EM. Although some complexes show similar behaviour in two of the solvents, there is no consistency across all of the complexes in all three solvents studied. The determination of EM factors out solvent effects on H-bond strength and the zinc porphyrin–pyridine interaction, so these variations must be due to changes in the stability of the solvation shell as a whole. These results highlight the complexity of solvation phenomena, and the collection of a large body of experimental data on these relatively simple model systems should prove useful for the development of reliable simulation techniques for tackling more complex molecular recognition processes in solution.

Experimental

NMR titrations

NMR titrations were carried out by preparing a 2 ml sample of host at known concentration (10–13 mM). Then, 0.6 ml of this solution was removed, and a ^{1}H NMR spectrum was recorded. A 1 ml solution of guest (3500 mM) was prepared using the host solution, so that the concentration of host remained constant throughout the titration. Aliquots of guest solution were added successively to the NMR tube containing the host, and the NMR spectrum was recorded after each addition. Changes in chemical shift were analyzed by fitting to a 1 : 1 binding isotherm in Microsoft Excel. Each titration was repeated at least three times, and the experimental error is quoted as twice the standard deviation.

UV/Vis absorption titrations

UV/Vis titrations were carried out by preparing a 10 ml sample of porphyrin at known concentration (4–7 μM) in spectroscopic grade solvent. A 10 ml solution of ligand (20–350 mM) was prepared using spectroscopic grade solvent. The porphyrin solution (150 μl) was added to a Hellma quartz 96 well plate, and UV/Vis spectra were recorded using a BMG FLUOstar Omega plate reader. Aliquots of ligand solution (3, 6 or 10 μl) were added successively to the wells containing the porphyrin solutions, and the UV/Vis spectra were recorded after each addition. Changes in absorbance were fit to a 1 : 1 binding isotherm in Microsoft Excel to obtain the association constant. Each titration was repeated at least three times, and the experimental error is quoted as twice the standard deviation.

We thank the Royal Society for a Newton International Fellowship (EC).

Notes and references

1 (*a*) J. Rebek, *Acc. Chem. Res.*, 1990, **23**, 399–404; (*b*) E. A. Meyer, R. K. Castellano and F. Diederich, *Angew. Chem., Int. Ed.*, 2003, **42**, 1210–1250; (*c*) H. J. Schneider, *Chem. Soc. Rev.*, 1994, **23**, 227–234; (*d*) J. C. Ma and D. A. Dougherty, *Chem. Rev.*, 1997, **97**, 1303–1324; (*e*) C. A. Hunter, K. R. Lawson, J. Perkins and C. J. Urch, *J. Chem. Soc., Perkin Trans. 2*, 2001, 651–669; (*f*) S. Paliwal, S. Geib and C. S. Wilcox, *J. Am. Chem. Soc.*, 1994, **116**, 4497–4498.

2 (*a*) W. L. Jorgensen and J. Pranata, *J. Am. Chem. Soc.*, 1990, **112**, 2008–2010; (*b*) T. J. Murray and S. C. Zimmerman, *J. Am. Chem. Soc.*, 1992, **114**, 4010–4011; (*c*) J. Sartorius and H. J. Schneider, *Chem.–Eur. J.*, 1996, **2**, 1446–1452.

3 (*a*) J. C. Adrian and C. S. Wilcox, *J. Am. Chem. Soc.*, 1989, **111**, 8055–8057; (*b*) R. P. Bonarlaw and J. K. M. Sanders, *J. Am. Chem. Soc.*, 1995, **117**, 259–271; (*c*) K. T. Chapman and W. C. Still, *J. Am. Chem. Soc.*, 1989, **111**, 3075–3077; (*d*) B. R. Linton, M. S. Goodman, E. Fan, S. A. van Arman and A. D. Hamilton, *J. Org. Chem.*, 2001, **66**, 7313–7319; (*e*) R. M. Grotzfeld, N. Branda and J. Rebek, *Science*, 1996, **271**, 487–489; (*f*) R. Meissner, X. Garcias, S. Mecozzi and J. Rebek, *J. Am. Chem. Soc.*, 1997, **119**, 77–85; (*g*) Y. Tokunaga, D. M. Rudkevich, J. Santamaria, G. Hilmersson and J. Rebek, *Chem.–Eur. J.*, 1998, **4**, 1449–1457; (*h*) S. B. Ferguson, E. M. Sanford, E. M. Seward and F. Diederich, *J. Am. Chem. Soc.*, 1991, **113**, 5410–5419; (*i*) G. A. Breault, C. A. Hunter and P. C. Mayers, *J. Am. Chem. Soc.*, 1998, **120**, 3402–3410.

4 (*a*) J. K. Sprafke, B. Odell, T. D. W. Claridge and H. L. Anderson, *Angew. Chem., Int. Ed.*, 2011, **50**, 5572–5575; (*b*) A. Camara-Campos, C. A. Hunter and S. Tomas, *Proc. Natl. Acad. Sci. U. S. A.*, 2006, **103**, 3034–3038; (*c*) E. Chekmeneva, C. A. Hunter, M. J. Packer and S. M. Turega, *J. Am. Chem. Soc.*, 2008, **130**, 17718–17725; (*d*) C. A. Hunter, N. Ihekwaba, M. C. Misuraca, M. D. Segarra-Maset and S. M. Turega, *Chem. Commun.*, 2009, 3964–3966; (*e*) V. M. Krishnamurthy, V. Semetey, P. J. Bracher, N. Shen and G. M. Whitesides, *J. Am. Chem. Soc.*, 2007, **129**, 1312–1320; (*f*) S. L. Tobey and E. V. Anslyn, *J. Am. Chem. Soc.*, 2003, **125**, 10963–10970; (*g*) J. H. Rao, J. Lahiri, L. Isaacs, R. M. Weis and G. M. Whitesides, *Science*, 1998, **280**, 708–711.

5 (*a*) F. Battistini, C. A. Hunter, E. Gardiner and M. J. Packer, *J. Mol. Biol.*, 2010, **396**, 264–279; (*b*) T. F. A. De Greef, M. M. J. Smulders, M. Wolffs, A. P. H. J. Schenning, R. P. Sijbesma and E. W. Meijer, *Chem. Rev.*, 2009, **109**, 5687–5754; (*c*) M. S. Taylor and E. N. Jacobsen, *Angew. Chem., Int. Ed.*, 2006, **45**, 1520–1543; (*d*) T. Akiyama, J. Itoh and K. Fuchibe, *Adv. Synth. Catal.*, 2006, **348**, 999–1010.

6 G. Chessari, C. A. Hunter, C. M. R. Low, M. J. Packer, J. G. Vinter and C. Zonta, *Chem.–Eur. J.*, 2002, **8**, 2860–2867.

7 (*a*) C. A. Hunter, M. C. Misuraca and S. M. Turega, *J. Am. Chem. Soc.*, 2011, **133**, 582–594; (*b*) C. A. Hunter, M. C. Misuraca and S. M. Turega, *Chem. Sci.*, 2012, **3**, 589–601; (*c*) C. A. Hunter, M. C. Misuraca and S. M. Turega, *J. Am. Chem. Soc.*, 2011, **133**, 20416–20425.

8 (*a*) C. A. Hunter, *Angew. Chem., Int. Ed.*, 2004, **43**, 5310–5324; (*b*) M. H. Abraham and J. A. Platts, *J. Org. Chem.*, 2001, **66**, 3484–3491.

9 R. Cabot and C. A. Hunter, *Chem. Soc. Rev.*, 2012, in press.

10 (*a*) A. Horovitz and A. R. Fersht, *J. Mol. Biol.*, 1990, **214**, 613–617; (*b*) S. L. Cockroft and C. A. Hunter, *Chem. Soc. Rev.*, 2007, **36**, 172–188; (*c*) A. Camara-Campos, D. Musumeci, C. A. Hunter and S. Turega, *J. Am. Chem. Soc.*, 2009, **131**, 18518–18524.

11 (*a*) C. A. Hunter and H. L. Anderson, *Angew. Chem., Int. Ed.*, 2009, **48**, 7488–7499; (*b*) G. Ercolani, C. Piguet, M. Borkovec and J. Hamacek, *J. Phys. Chem. B*, 2007, **111**, 12195–12203; (*c*) C. Galli and L. Mandolini, *Eur. J. Org. Chem.*, 2000, 3117–3125; (*d*) A. R. Fersht and A. J. Kirby, *J. Am. Chem. Soc.*, 1967, **89**, 4857; (*e*) A. J. Sinclair, V. del Amo and D. Philp, *Org. Biomol. Chem.*, 2009, **7**, 3308–3318; (*f*) X. L. Chi, A. J. Guerin, R. A. Haycock, C. A. Hunter and L. D. Sarson, *Chem. Commun.*, 1996, 885–885.